Neuroligins/LRRTMs prevent activity- and Ca^{2+}/calmodulin-dependent synapse elimination in cultured neurons

Jaewon Ko,[1] Gilberto J. Soler-Llavina,[3] Marc V. Fuccillo,[1,3] Robert C. Malenka,[3] and Thomas C. Südhof[1,2]

[1]Department of Molecular and Cellular Physiology, [2]Howard Hughes Medical Institute, and [3]Nancy Pritzker Laboratory, Department of Psychiatry and Behavioral Sciences, Stanford University School of Medicine, Stanford, CA 94305

Neuroligins (NLs) and leucine-rich repeat transmembrane proteins (LRRTMs) are postsynaptic cell adhesion molecules that bind to presynaptic neurexins. In this paper, we show that short hairpin ribonucleic acid–mediated knockdowns (KDs) of LRRTM1, LRRTM2, and/or NL-3, alone or together as double or triple KDs (TKDs) in cultured hippocampal neurons, did not decrease synapse numbers. In neurons cultured from NL-1 knockout mice, however, TKD of LRRTMs and NL-3 induced an ∼40% loss of excitatory but not inhibitory synapses. Strikingly, synapse loss triggered by the LRRTM/NL deficiency was abrogated by chronic blockade of synaptic activity as well as by chronic inhibition of Ca^{2+} influx or Ca^{2+}/calmodulin (CaM) kinases. Furthermore, postsynaptic KD of CaM prevented synapse loss in a cell-autonomous manner, an effect that was reversed by CaM rescue. Our results suggest that two neurexin ligands, LRRTMs and NLs, act redundantly to maintain excitatory synapses and that synapse elimination caused by the absence of NLs and LRRTMs is promoted by synaptic activity and mediated by a postsynaptic Ca^{2+}/CaM-dependent signaling pathway.

Introduction

Synapse assembly, maturation, validation, and maintenance are thought to depend on trans-synaptic cell adhesion molecules, including neurexins, neuroligins (NLs), and leucine-rich repeat transmembrane proteins (LRRTMs; Ushkaryov et al., 1992; Ichtchenko et al., 1995; Laurén et al., 2003). Four NLs are expressed throughout the brain but are differentially targeted within neurons to specific synapses. NL1 is specific for excitatory and NL2 for inhibitory synapses, whereas NL3 appears to be present in both types of synapses, and NL4 is expressed at low levels in as yet uncharacterized locations (Song et al., 1999; Graf et al., 2004; Varoqueaux et al., 2004, 2006; Budreck and Scheiffele, 2007). LRRTMs are also produced from four genes but with distinct regional expression patterns (Laurén et al., 2003). For example, the CA1 region of the hippocampus expresses only LRRTM1 and LRRTM2 at significant levels, whereas the dentate gyrus produces all four LRRTM isoforms (Laurén et al., 2003). Interestingly, NL1, NL3, NL4, and LRRTM3 have been implicated in autism (Südhof, 2008; Sousa et al., 2010), and LRRTM1 has been linked to schizophrenia (Francks et al., 2007).

NLs and LRRTMs both potently increase synapse density when overexpressed in neurons, suggesting that they are involved in synapse formation or maintenance (Chih et al., 2005; Chubykin et al., 2007; Ko et al., 2009a,b). LRRTMs bind to presynaptic neurexins, raising the intriguing possibility that LRRTMs and NLs might be redundant postsynaptic neurexin ligands for trans-synaptic cell adhesion (de Wit et al., 2009; Ko et al., 2009b; Siddiqui et al., 2010). Moreover, single short hairpin RNA (shRNA)–dependent knockdowns (KDs) of individual NLs and of LRRTM2 were reported to cause significant synapse loss (Chih et al., 2005; de Wit et al., 2009), indicating that NLs and LRRTMs are both separately required to initiate synapse formation. Surprisingly, however, deletion of NLs in

Correspondence to Jaewon Ko: jaewonko@yonsei.ac.kr; or Thomas C. Südhof: tcs1@stanford.edu

J. Ko's present address is Dept. of Biochemistry, College of Life Science and Biotechnology, Yonsei University, Seodaemun-gu, Seoul 120-749, South Korea.

Abbreviations used in this paper: AMPA, 2-amino-3-(5-methyl-3-oxo-1,2,-oxazol-4-yl) propanoic acid; ANOVA, analysis of variance; APV, DL-2-amino-5-phosphonovalerate; DIV, day in vitro; DKD, double KD; EPSC, excitatory postsynaptic current; IPSC, inhibitory postsynaptic current; KD, knockdown; KO, knockout; LRRTM, leucine-rich repeat transmembrane protein; NBQX, 2,3-Dioxo-6-nitro-1,2,3,4-tetrahydrobenzo[f]quinoxaline-7-sulfonamide; NL, neuroligin; NMDA, *N*-methyl-D-aspartate; shRNA, short hairpin RNA; TKD, triple KD; TTX, tetrodotoxin; VGAT, vesicular γ-aminobutyric acid transporter.

© 2011 Ko et al. This article is distributed under the terms of an Attribution–Noncommercial–Share Alike–No Mirror Sites license for the first six months after the publication date (see http://www.rupress.org/terms). After six months it is available under a Creative Commons License (Attribution–Noncommercial–Share Alike 3.0 Unported license, as described at http://creativecommons.org/licenses/by-nc-sa/3.0/).

The Rockefeller University Press $30.00
J. Cell Biol. Vol. 194 No. 2 323–334
www.jcb.org/cgi/doi/10.1083/jcb.201101072

THE JOURNAL OF CELL BIOLOGY

Downloaded from http://rupress.org/jcb/article-pdf/194/2/323/1894868/jcb_201101072.pdf by guest on 05 December 2025

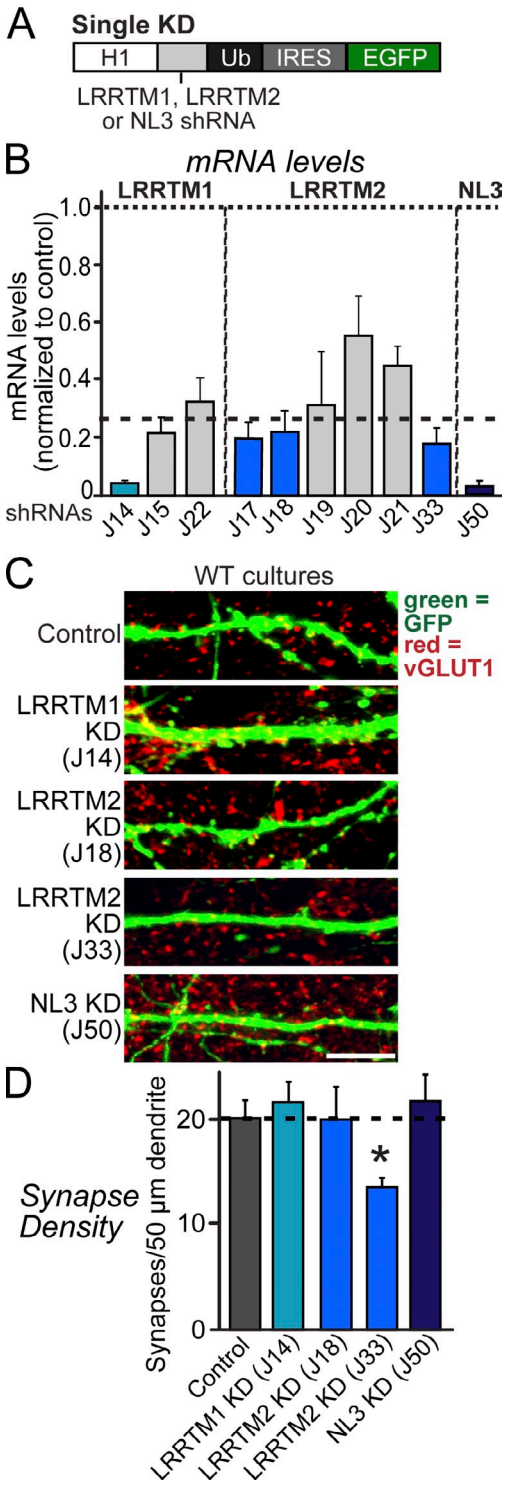

Figure 1. **Single KDs of LRRTMs or NLs do not alter synapse density in cultured neurons.** (A) Design of lentiviral shRNA vectors for KD of LRRTM1, LRRTM2, or NL3. H1, human H1 promoter; IRES, internal ribosome entry sequence; Ub, ubiquitin promoter. (B) Levels of target mRNAs (LRRTM1, LRRTM2, and NL3) measured by quantitative RT-PCR in cultured cortical neurons infected at DIV3 with lentiviruses expressing the indicated shRNAs. mRNAs were determined at DIV12 and 13. Dashed line, 75% KD cutoff level for tests of biological effects. (C) Representative images of cultured hippocampal neurons that were transfected at DIV3 with lentiviral vector lacking shRNA expression (control) or expressing shRNAs targeting LRRTM1 (J14), LRRTM2 (J18 and J33), or NL3 (J50). Neurons were analyzed at DIV14 by double immunofluorescence with antibodies to GFP and vGLUT1. WT, wild type. Bar, 5 µm. (D) A summary graph of the effects of single KD of LRRTM1, LRRTM2, and NL3 on excitatory synapse density, quantified using vGLUT1 immunoreactivity. The dotted line represents a control level of synapse density for comparisons with the other experimental conditions. (B and D) The shaded gray and blue bars represent the results with the non-effective and effective shRNA vectors, respectively. The data shown are means ± SEMs (n = 3 independent culture experiments). Statistical significance was assessed by comparing the various conditions with controls using the ANOVA Tukey's test. *, $P < 0.05$. For further data, see Figs. S1 and S2.

single, double, or triple knockout (KO) mice or deletion of LRRTM1 in single KO mice failed to produce significant synapse loss (Varoqueaux et al., 2006; Linhoff et al., 2009). This finding, together with the observation that the synapse-boosting effect of overexpressed NLs requires synaptic activity (Chubykin et al., 2007), prompted an alternative hypothesis, namely that NLs and LRRTMs function as signaling molecules that translate synaptic activity into synapse maintenance (i.e., validate synapses; Südhof, 2008).

Here, we systematically tested the effects of decreased LRRTM and NL expression on synapse numbers in cultured hippocampal neurons. Consistent with the KO results, we find that individual or combined KDs of the two LRRTMs that are highly expressed in the hippocampus (LRRTM1 and LRRTM2) or KD of NL3 alone did not decrease synapse numbers in wild-type neurons. However, the combined triple KD (TKD) of LRRTM1, LRRTM2, and NL3 in NL1 KO neurons caused a robust decline in excitatory synapse density. This synapse loss was reversed by reexpression of full-length NL1 or LRRTM2 as well as by expression of the extracellular regions of NL1 or LRRTM2. Importantly, both the increases in synapse numbers by gain-of-function and the decreases in synapse numbers by loss-of-function manipulations of NLs and LRRTMs were counteracted by blocking synaptic activity. Collectively, these results suggest that NLs and LRRTMs cooperate to maintain normal levels of excitatory synapses in an activity-dependent manner and that neurexins are presynaptic hub molecules that coordinate postsynaptic signals from independent ligands.

Results

Lentiviral KDs of LRRTMs or NL3 do not suppress synapse numbers

To identify effective shRNAs for KD of LRRTM1, LRRTM2, and NL3, we expressed shRNAs in cultured mouse cortical neurons using lentiviruses and quantified endogenous target mRNA levels by real-time RT-PCR (Figs. 1 A and S1). We identified shRNAs that suppress endogenous mRNAs for LRRTM1 by ~90% (J14), for LRRTM2 by ~75% (J17, J18, and J33), and for NL3 by ~95% (J50; Fig. 1 B). Moreover, we confirmed that the NL3 shRNA severely suppressed NL3 protein expression (Fig. S1), although we could not measure LRRTM protein levels because of a lack of LRRTM antibodies.

Next, we investigated whether single KD of LRRTM1, LRRTM2, or NL3 alters synapse density in cultured neurons. We transfected cultured hippocampal neurons at day in vitro 3 (DIV3) with vectors that express only EGFP (control) or coexpress

Downloaded from http://rupress.org/jcb/article-pdf/194/2/323/1894868/jcb_201101072.pdf by guest on 05 December 2025

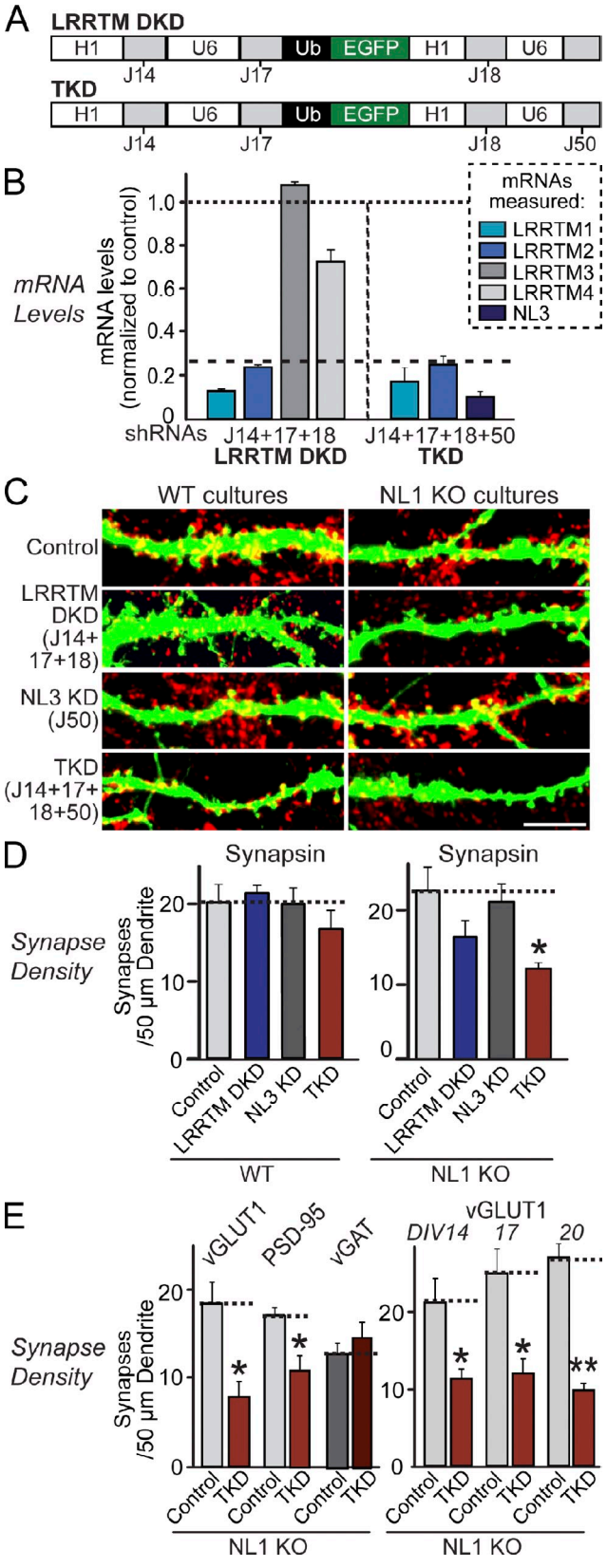

Figure 2. **Combined loss of function of LRRTM1, LRRTM2, NL1, and NL3 causes synapse loss.** (A) Design of lentiviral shRNA vectors for simultaneous KD of multiple targets using the indicated shRNAs. H1 and U6, human H1 and U6 promoters; Ub, ubiquitin promoter. Note that two LRRTM2 shRNAs (J17 and J18) were used simultaneously for efficient KD; J33 was excluded because of its apparent off-target effect. (B) Measurements of target mRNA levels (LRRTM1, LRRTM2, and NL3) in cultured cortical neurons as described in Fig. 1 B, except that neurons were infected with DKD lentiviruses expressing shRNAs to LRRTM1 and LRRTM2 or TKD lentiviruses that additionally express an shRNA to NL3. The target mRNA measured is color coded as indicated on the right. Dashed line, 75% KD cutoff level for tests of biological effects. (C) Representative images of hippocampal neurons cultured from wild-type (WT) or NL1 KO mice that were transfected with the indicated KD vectors at DIV9 and analyzed by double immunofluorescence with antibodies to GFP and synapsin at DIV14. For transfections at DIV3, see Fig. S2. Bar, 5 µm. (D) Summary graphs of the effect in wild-type (left) or NL1 KO neurons (right) of the LRRTM DKD, the NL3 KD, and the combined LRRTM1, LRRTM2, and NL3 TKD on overall synapse densities, quantified using synapsin immunoreactivity. (E) Summary graphs of the effect of the LRRTM1, LRRTM2, and NL3 TKD in NL1 KO neurons on the density of excitatory synapses (measured using vGLUT1 or PSD-95 as markers) or inhibitory synapses (using vGAT as a marker) determined at DIV14 (left) or of the effect of the TKD on excitatory synapse density monitored with vGLUT1 as a marker after longer culture times, comparing DIV14 with DIV17 and DIV20 (right). (B, D, and E) The dotted lines represent control levels for comparisons with the other experimental conditions. The data shown are means ± SEMs (n = 3 independent culture experiments). Statistical significance was assessed by comparing the various conditions with controls using the ANOVA Tukey's test. *, $P < 0.05$. For additional images and synapse size quantitations and different variations of the KD experiments, see Figs. S2 and S3. For analysis of the TKD effect on neuronal morphology and differentiation, see Fig. S3.

EGFP with shRNAs against LRRTM1, LRRTM2, or NL3. We immunostained the transfected neurons at DIV14 for vGLUT1, an excitatory presynaptic marker, and quantified the density and size of excitatory synapses on dendrites of the transfected neurons (Figs. 1 [C and D] and S2). None of the shRNAs decreased the excitatory synapse density, except for one of the LRRTM2 shRNAs (J33). Similar results were obtained when we infected hippocampal neurons with lentiviruses expressing shRNAs at DIV3 or when we transfected cultured hippocampal neurons at DIV9 (Fig. S2, A and B). The J33 shRNA, which was the only shRNA that by itself decreased synapse density, is identical to an shRNA used previously to demonstrate that the LRRTM2 KD decreases synapse numbers (de Wit et al., 2009), thus confirming these results. However, other LRRTM2 shRNAs that produce a similar KD of LRRTM2 expression did not change synapse numbers (Fig. 1 B), suggesting that the J33 effect may be mediated by an off-target mechanism (Alvarez et al., 2006).

KD of both LRRTMs and NL3 in NL1 KO neurons reduces excitatory synapse numbers

We next generated expression vectors that contain four human polymerase III promoters (to express shRNAs) and a ubiquitin promoter (to express EGFP for visualization of infected or transfected neurons; Fig. 2 A). We then suppressed expression of LRRTM1 and LRRTM2 with this vector (denoted as LRRTM double KD [DKD]; note that the two LRRTM2 shRNAs without off-target effects [J17 and J18] were used together here to increase the KD efficiency). For simultaneous KD of LRRTMs and NL3, we additionally introduced the NL3 shRNA into the DKD vector and found that mRNA levels of all three proteins (LRRTM1, LRRTM2, and NL3) were successfully suppressed (denoted as TKD; Fig. 2, A and B).

Downloaded from http://rupress.org/jcb/article-pdf/194/2/323/1894868/jcb_201101072.pdf by guest on 05 December 2025

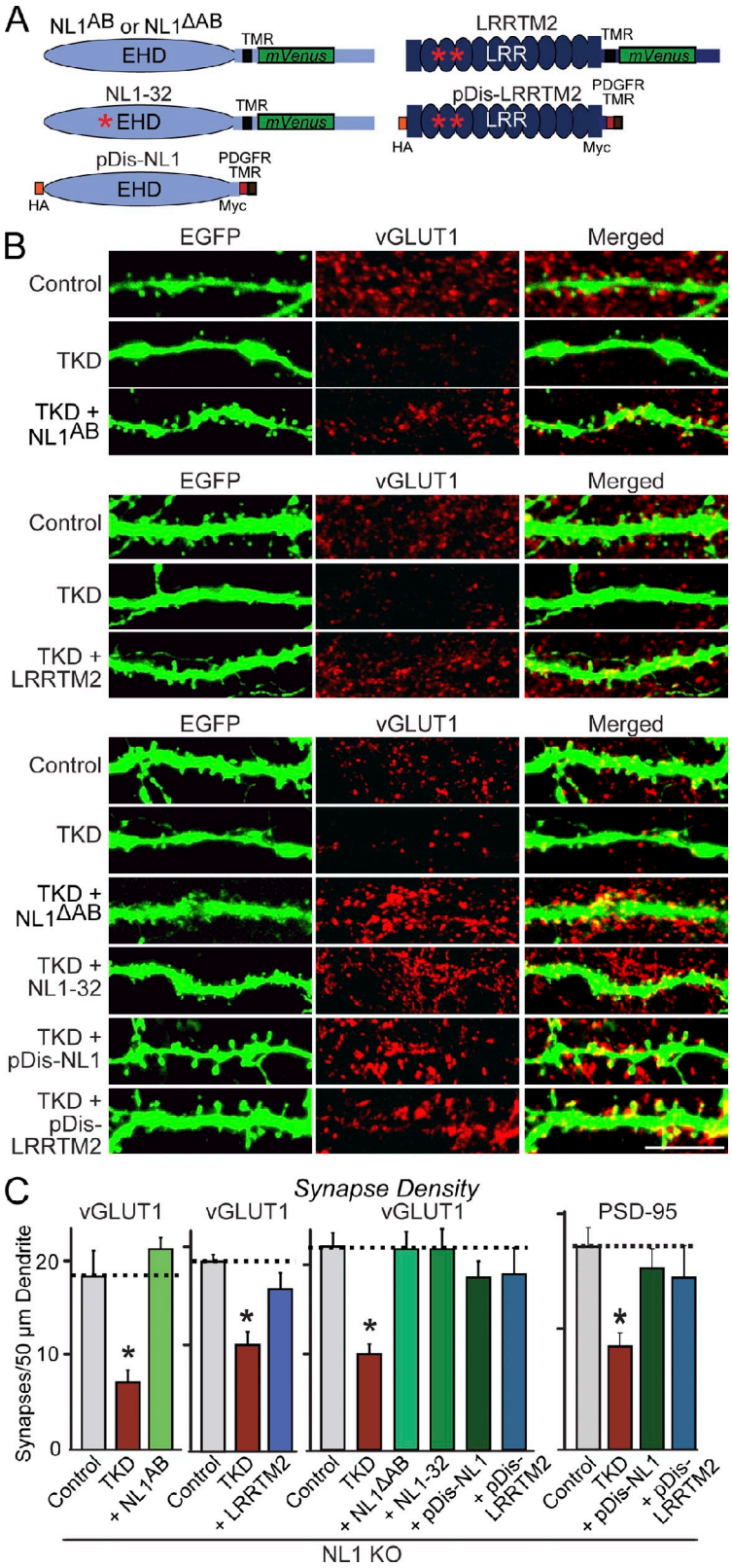

Figure 3. **Reversal of synapse loss by overexpression of LRRTM2 or NL1 in LRRTM/NL-deficient neurons.** (A) Diagrams of proteins expressed from shRNA-resistant transcripts in neurons. Full-length proteins contain an mVenus tag in the cytoplasmic tail; two splice variants of NL1 containing or lacking inserts in splice sites A and B (Boucard et al., 2005) were used as indicated. NL1-32 carries point mutations that block neurexin binding (indicated by asterisks; Ko et al., 2009a). In pDis proteins, the transmembrane region (TMR) and cytoplasmic sequence of NL1 or LRRTM2 are replaced with the transmembrane region of the PDGF receptor (PDGFR). EHD, esterase homology domain; LRR, leucine-rich repeat; HA and Myc, HA and myc epitopes. (B) Representative images of cultured hippocampal neurons from NL1 KO mice that were transfected with vectors expressing EGFP alone (control) or together with the indicated shRNAs (TKD; triple LRRTM1, LRRTM2, and NL3 KD). shRNA vectors were cotransfected at DIV9 with plasmids encoding the indicated proteins. Neurons were analyzed by double immunofluorescence with antibodies to GFP and vGLUT1 at DIV14. Bar, 5 µm. (C) Summary graphs of synapse densities. The dotted lines represent control levels for comparisons with the other experimental conditions. The data shown are means ± SEMs (n = 3 independent culture experiments). Statistical significance was assessed by comparing the various conditions with controls using the ANOVA Tukey's test. *, $P < 0.05$.

Using the DKD and TKD vectors, we examined whether LRRTMs alone or together with NL3 are essential for synapse maintenance. To include NL1 in our analysis, we additionally performed all experiments in neurons cultured from NL1 KO mice (Varoqueaux et al., 2006). We did not include NL2 and NL4 in this study because NL2 localizes to inhibitory synapses (Graf et al., 2004; Varoqueaux et al., 2004; Chubykin et al., 2007; Poulopoulos et al., 2009), and NL4 is expressed only at very low levels (Varoqueaux et al., 2006).

Strikingly, neither the DKD of LRRTM1 and LRRTM2 nor the TKD of these LRRTMs together with NL3 significantly decreased synapse numbers in wild-type hippocampal neurons

Downloaded from http://rupress.org/jcb/article-pdf/194/2/323/1894868/jcb_201101072.pdf by guest on 05 December 2025

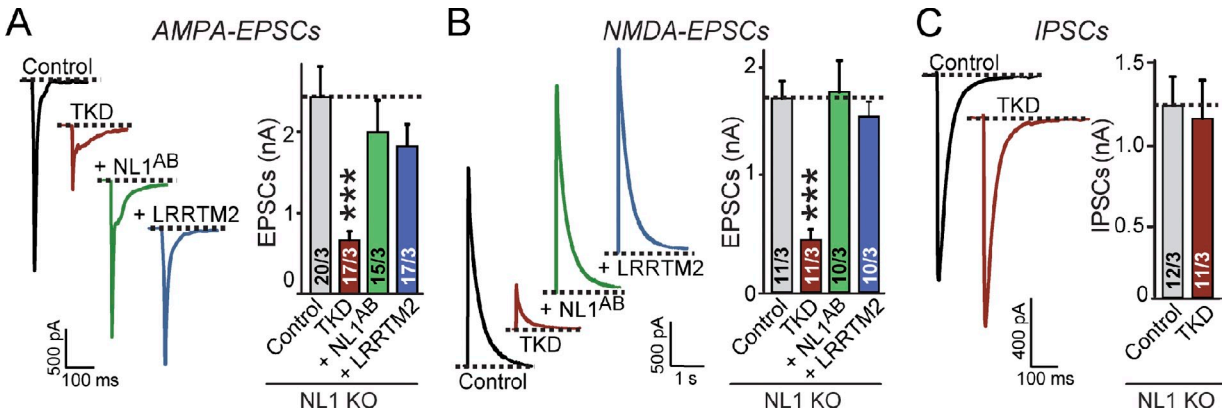

Figure 4. **Combined loss of function of LRRTM1, LRRTM2, NL1, and NL3 selectively impairs excitatory synaptic transmission: reversal by overexpression of LRRTM2 or NL1.** (A) Representative traces (left) and summary graphs of the amplitudes (right) of evoked AMPA receptor–mediated EPSCs in NL1 KO neurons infected with lentiviruses that express only EGFP (control) and coexpress EGFP with the LRRTM1, LRRTM2, and NL3 shRNAs without (TKD) or with coexpression of either NL1 containing inserts in splice sites A and B (+NL1^{AB}) or of LRRTM2 (+LRRTM2). (B) Same as A, except that evoked NMDA receptor–mediated EPSCs were measured. (C) Same as A, except that evoked IPSCs were measured, and only the control and TKD conditions were examined because the TKD had no effect on inhibitory responses. (A–C) The dotted lines represent control levels for comparisons with the other experimental conditions. The data shown are means ± SEMs (numbers in bars = numbers of cells/cultures analyzed). Statistical significance was assessed by comparing the various conditions with controls using unpaired, two-tailed Student's *t* tests. ***, $P < 0.001$.

(Figs. 2 [C–E] and S2). When we introduced the DKD into NL1 KO neurons (which also exhibit no synapse loss), we observed a small but nonsignificant decrease in synapse numbers. Only introduction of the LRRTM/NL TKD into NL1 KO neurons caused a robust decrease in synapse density (~40–50%, depending on whether pre- or postsynaptic markers were analyzed; Fig. 2, C–E) without changing the size, dendrite length, or dendritic branching of the neurons (Fig. S3, A and B). The synapse loss in NL1 KO neurons expressing the TKD plasmids was specific for excitatory synapses (Fig. 2 E), consistent with the selective effects of the targeted proteins in gain-of-function assays (de Wit et al., 2009; Ko et al., 2009b). In our culture system, neurons continue to form synapses until at least 3 wk in vitro. The TKD-induced synapse loss in NL1 KO neurons was observed independent of the age of the culture (Figs. 2 E and S3 [C and D]) and could reflect diminished synapse formation and/or increased synapse elimination. Together, these results suggest that LRRTMs and NLs redundantly maintain excitatory synapses in cultured hippocampal neurons. Note that, in these experiments, the analyzed neurons represent a small subset of all neurons that are surrounded by nontransfected neurons; thus, the KD neurons compete with control neurons for synaptic inputs. However, the same results were obtained for LRRTM DKDs in experiments in which neurons were infected with lentiviruses expressing the KD shRNAs, and, thus, no competition between neurons for synaptic inputs exists (Fig. S2 B).

Reversal of the TKD phenotype in NL1 KO neurons by LRRTM2 or NL1 independent of their intracellular sequences

Next, we cotransfected into NL1 KO neurons the TKD plasmid with plasmids encoding full-length NL1 or LRRTM2 or their extracellular sequences fused to the PDGF receptor transmembrane region (Fig. 3 A). Expression of both full-length NL1 or LRRTM2 restored excitatory synapse numbers (Fig. 3, B and C), explaining the lack of a TKD phenotype in wild-type neurons that still express endogenous NL1 (Fig. 2, C and D). Moreover, expression of only the extracellular sequences of NL1 or LRRTM2 also reversed the TKD phenotype in NL1 KO neurons and restored the density of vGLUT1- and PSD-95–containing synapses to control levels (Fig. 3, B and C). Furthermore, an NL1 mutant that lacks neurexin-binding activity (NL1-32) was still active. These results are consistent with previous observations that found when overexpressed, the extracellular region of NL1 is sufficient to increase excitatory synapse density, as is the NL1-32 mutant (Chubykin et al., 2007; Ko et al., 2009a).

To determine whether the changes in anatomical synapse numbers reflect the changes in the number of functional synapses, we examined synaptic transmission in NL1 KO neurons that were infected with control viruses or the TKD viruses either alone or together with the NL1 or LRRTM2 expression vectors (Fig. 4). Measurements of 2-amino-3-(5-methyl-3-oxo-1,2,-oxazol-4-yl) propanoic acid (AMPA) and of *N*-methyl-D-aspartate (NMDA) receptor–mediated excitatory postsynaptic currents (EPSCs) using the protocol of Maximov et al. (2007) showed that the TKD caused a massive decrease in excitatory synaptic transmission, with both glutamate receptor components affected equally (Fig. 4, A and B). Expression of either NL1 or of LRRTM2 reversed this impairment. In contrast, the TKD did not alter inhibitory postsynaptic currents (IPSCs), confirming its specificity (Fig. 4 C).

Synaptic activity is required for synapse loss in LRRTM/NL-deficient neurons

Because chronic inhibition of NMDA receptors or of Ca^{2+}/CaM-dependent kinase (CaM kinase) suppresses the synapse-boosting activities of overexpressed NL1 in cultured neurons (Chubykin et al., 2007), we next explored whether a similar activity dependence applies to the synapse-boosting effect of overexpressed LRRTM2. We transfected neurons at DIV10 with expression vectors encoding mVenus (control), mVenus-fused NL1$^{\Delta AB}$ (lacking inserts in splice sites A and B), and

Downloaded from http://rupress.org/jcb/article-pdf/194/2/323/1894868/jcb_201101072.pdf by guest on 05 December 2025

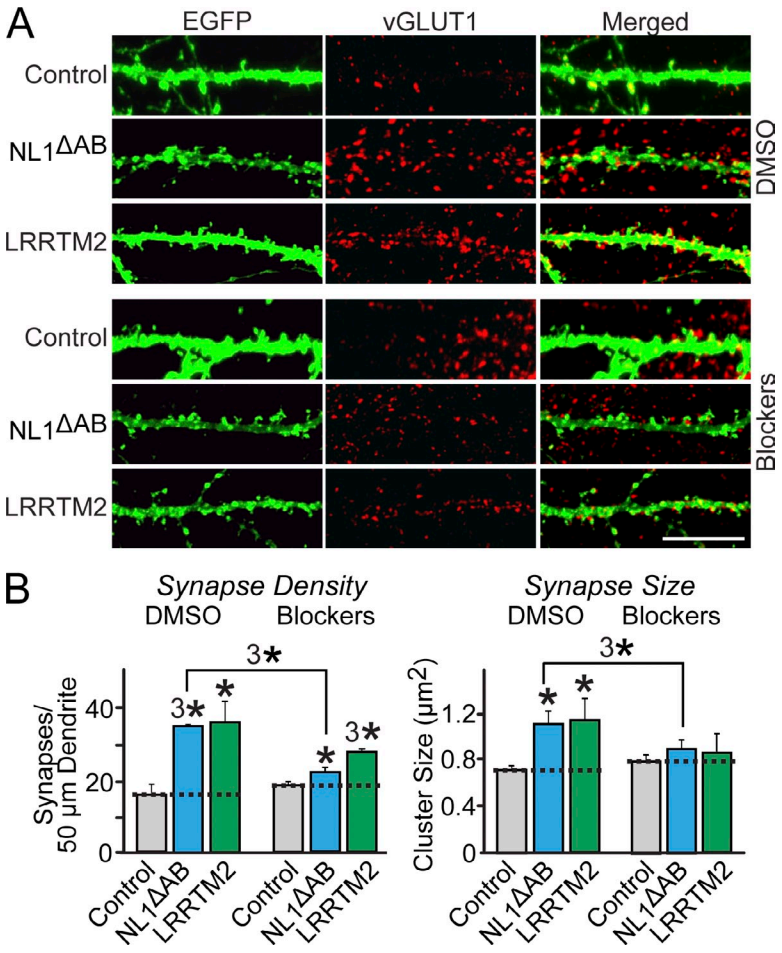

Figure 5. **Activity-dependent synapse formation induced by overexpression of NL1 or LRRTM2 in neurons.** (A) Representative images of cultured wild-type hippocampal neurons that were transfected at DIV10 with expression plasmids encoding mVenus (control) or mVenus fusion proteins of NL1 lacking inserts in splice sites A and B ($NL1^{\Delta AB}$) or of LRRTM2 and analyzed at DIV14 by double immunofluorescence with antibodies to GFP and vGLUT1. DMSO (negative control) or a cocktail of blockers for all neurotransmitter receptors (50 µM APV + 20 µM NBQX + 50 µM picrotoxin + 10 µM LY341495) was added to the cultured neurons at the time of transfection to block synaptic activity. Bar, 5 µm. (B) Summary graphs of the effect of the synaptic activity blockers on synapse density and synapse size in transfected neurons, quantified by vGLUT1 staining. The dotted lines represent control levels for comparisons with the other experimental conditions. The statistics in B were performed in comparison with DMSO-treated conditions, determined by the ANOVA Tukey's test. *, $P < 0.05$; ^{3}*, $P < 0.001$.

mVenus-fused LRRTM2. We subsequently treated the transfected neurons from the time of transfection with either DMSO or a cocktail of neurotransmitter receptor inhibitors to block synaptic activity (a mixture of DL-2-amino-5-phosphonovalerate [APV], 2,3-Dioxo-6-nitro-1,2,3,4-tetrahydrobenzo[f]quinoxaline-7-sulfonamide [NBQX], picrotoxin, and LY341495 [a type II metabotropic glutamate receptor antagonist]) and immunostained the neurons at DIV14. As previously described, overexpression of both $NL1^{\Delta AB}$ and LRRTM2 increased excitatory synapse numbers and sizes (Boucard et al., 2005; de Wit et al., 2009; Ko et al., 2009a,b). Upon blockade of synaptic activity, overexpression of NL1 and LRRTM2 was less effective in increasing synapse densities and no longer increased synapse sizes (Fig. 5).

We then examined whether synapse elimination induced by the TKD in NL1 KO neurons is also dependent on synaptic activity. Chronic treatment of control NL1 KO neurons with the neurotransmitter receptor inhibitor cocktail had no effect on synapse numbers, whereas the same treatment blocked the synapse loss induced by the TKD in NL1 KO neurons (Figs. 6 [A and B] and S4 A). These results were confirmed using both presynaptic (vGLUT1) and postsynaptic marker proteins (NMDAR1 and GluR2). Thus, both the increases in synapse numbers produced by NL1 or LRRTM2 overexpression and the decreases in synapse numbers produced by KD of LRRTMs and NL3 in NL1 KO neurons involve synaptic activity. Chronic stimulation of neurons by depolarization with 15 mM KCl did not increase the synapse loss caused by the TKD in NL1 KO neurons, indicating that the spontaneous synaptic activity in our cultures is sufficient to drive synapse elimination (Fig. S4, B and C).

In further experiments, we systematically tested specific receptor antagonists to identify the receptor activity that underlies the loss of synapses caused by NL and LRRTM KDs. Chronic treatment of control- or TKD-transfected NL1 KO neurons with DMSO (as a solvent control), APV, NBQX, picrotoxin, or LY341495 revealed that only the AMPA receptor antagonist NBQX prevented synapse loss in TKD neurons, whereas APV exerted a partial effect (Fig. 6, C and D). Conversely, tetrodotoxin (TTX), which selectively inhibits action potentials, was ineffective in blocking synapse loss, suggesting that spontaneous mini release is sufficient to activate synapse elimination in LRRTM/NL-deficient neurons. We observed no significant changes in synapse number in control neurons treated with individual drugs and no changes in synapse size under any condition tested (Fig. S5 A).

Activity-dependent synapse loss in LRRTM/NL-deficient neurons requires Ca^{2+} influx, CaM, and CaM kinase activity

A common mechanism by which activity influences synapse function is via Ca^{2+} and its downstream targets, such as CaM kinases (Wayman et al., 2008). Therefore, we explored the hypothesis that activity-dependent synapse loss may operate

Downloaded from http://rupress.org/jcb/article-pdf/194/2/323/1894868/jcb_201101072.pdf by guest on 05 December 2025

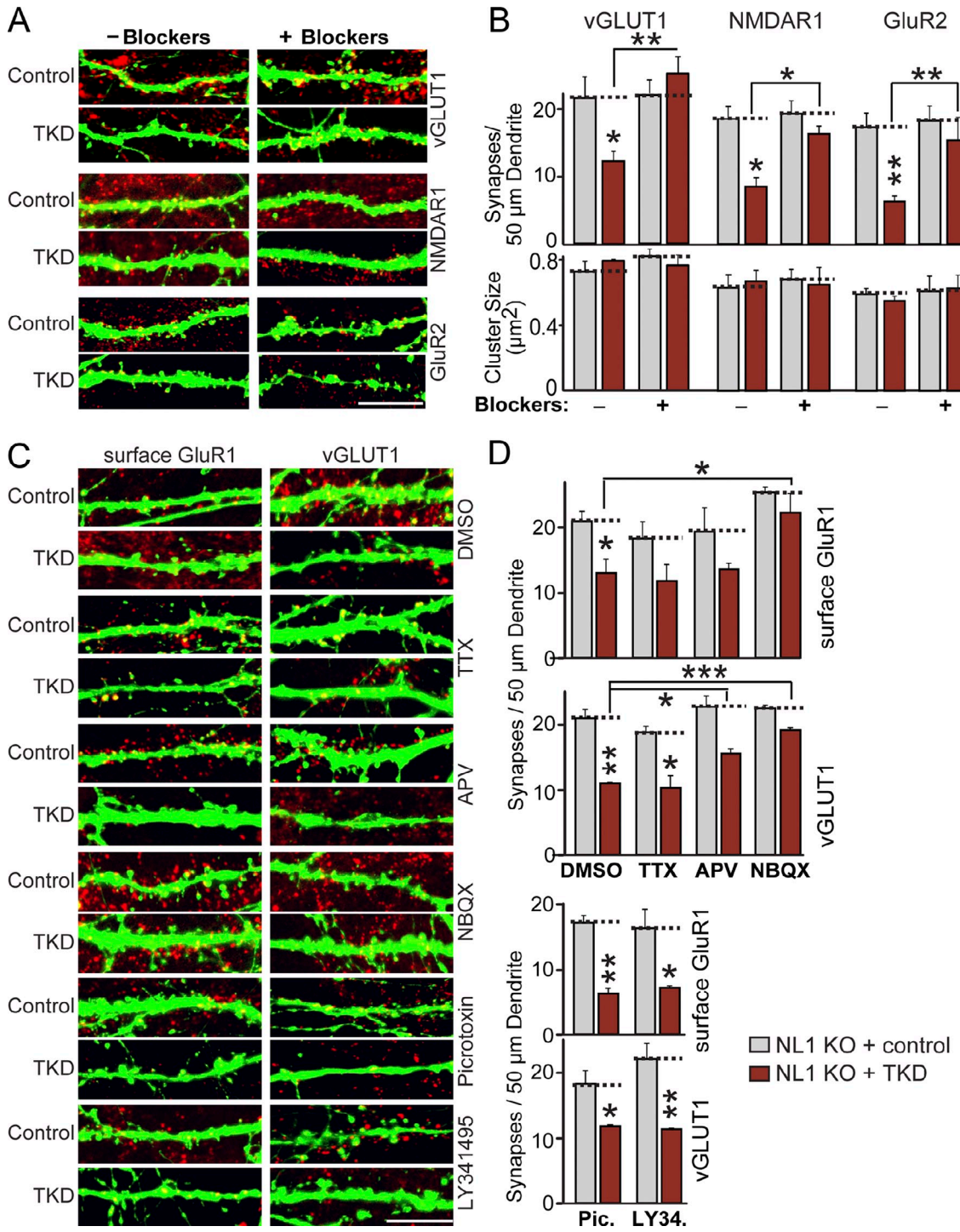

Figure 6. **Activity-dependent synapse elimination in LRRTM/NL-deficient neurons.** (A) Representative images of hippocampal neurons from NL1 KO mice that were transfected at DIV9 with a vector expressing EGFP only (control) or coexpressing the TKD shRNAs and analyzed at DIV14 by double immunofluorescence with antibodies to GFP and vGLUT1, NMDAR1, or GluR2 as indicated. Neurons were treated with DMSO (negative control) or a cocktail of blockers for all neurotransmitter receptors (50 µM APV + 20 µM NBQX + 50 µM picrotoxin + 10 µM LY341495) from the time of transfection to block synaptic activity. Only merged images are shown (vGLUT1, NMDAR1, or GluR2 in red and EGFP in green). See Fig. S5 for separate images. (B) A summary graph of the effects of the synaptic activity blockers on synapse density (top) and synapse size (bottom) in control and TKD neurons. (C) Representative images of hippocampal neurons from NL1 KO mice that were transfected at DIV9 with a vector expressing EGFP only (control) or coexpressing the TKD shRNAs and analyzed by double immunofluorescence with antibodies to GFP and vGLUT1 at DIV14. Neurons were treated separately with the agents indicated on the right (2 µM TTX, 50 µM APV, 20 µM NBQX, 50 µM picrotoxin, and 10 µM LY341495) and analyzed both by staining for surface-exposed postsynaptic GluR1 receptors (left) and for vGLUT1 (right). Only merged images are shown (surface GluR1 or vGLUT1 in red and EGFP in green). (D) Summary graphs of the effects of the LRRTM/NL TKD on synapse density as measured by staining for surface-exposed GluR1 and for vGLUT1 and of the effect of individual pharmacologic agents on the synapse loss produced by the TKD. (B and D) The dotted lines represent control levels for comparisons with the other experimental conditions. The data shown are means ± SEMs (n = 3 independent cultures). Statistical significance was assessed by comparing the various conditions with controls using the ANOVA Tukey's test. *, $P < 0.05$; **, $P < 0.01$; ***, $P < 0.001$. For analyses of synapse sizes, see Fig. S5. Bars, 5 µm.

Downloaded from http://rupress.org/jcb/article-pdf/194/2/323/1894868/jcb_201101072.pdf by guest on 05 December 2025

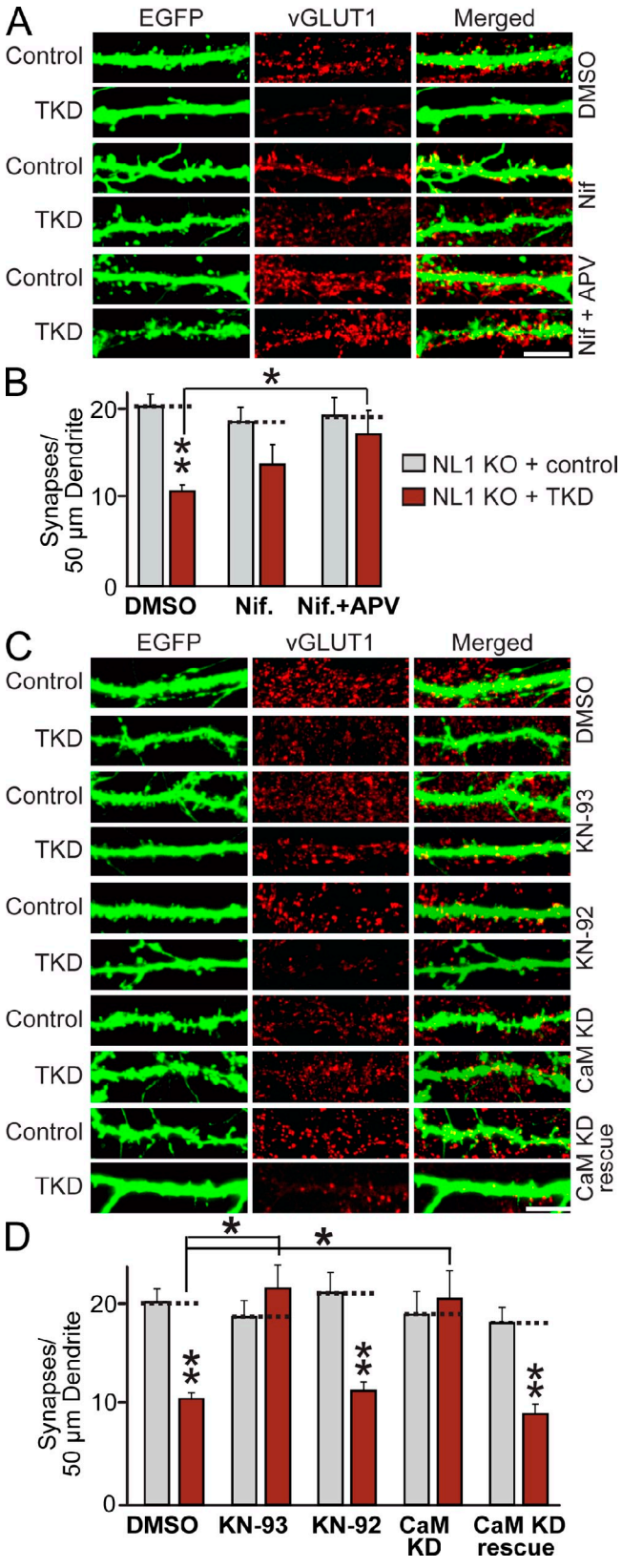

Figure 7. **Synapse elimination produced by combined loss of function of LRRTM1, LRRTM2, NL1, and NL3 requires Ca^{2+}/CaM signaling.** (A) Representative images of hippocampal neurons from NL1 KO mice that were transfected at DIV9 with lentiviruses expressing either EGFP alone (control) or together with the TKD shRNAs and analyzed by double immunofluorescence with antibodies to GFP and vGLUT1 at DIV14. Neurons were treated separately with the agents indicated on the right and analyzed with antibodies to GFP and vGLUT1. DMSO (negative control) or L-type calcium channel blocker and/or NMDA receptor antagonist (Nif = 10 µM nifedipine; Nif + APV = 10 µM nifedipine + 50 µM APV) were added to the cultured neurons at the time of transfection. Bar, 5 µm. (B) Summary graphs of the synapse density quantified in experiments as described in C. (C) Representative images of hippocampal neurons from NL1 KO mice that were transfected at DIV9 with lentiviruses expressing either EGFP alone (control) or together with the TKD shRNAs and analyzed by double immunofluorescence with antibodies to GFP and vGLUT1 at DIV14. Neurons were treated from DIV9 on with DMSO or 5 µM KN-93 or KN-92 (active and inactive CaM kinase inhibitor enantiomers) or were cotransfected with CaM KD shRNAs without (CaM KD) or with coexpression of shRNA-resistant full-length CaM (CaM KD rescue; Pang et al., 2010a). Neurons were analyzed at DIV14. Bar, 5 µm. (D) Summary graphs of the synapse density quantified in experiments as described in C. (B and D) The dotted lines represent control levels for comparisons with the other experimental conditions. The data shown are means ± SEMs (n = 3 independent culture experiments). Statistical significance was assessed using the ANOVA Tukey's test. *, $P < 0.05$; **, $P < 0.01$. For analyses of synapse sizes, see Fig. S5.

via a Ca^{2+}-dependent pathway involving CaM kinases that, in our cultured neurons, would be activated by AMPA receptor–dependent synaptic events. We found that inhibition of L-type Ca^{2+} channels with nifedipine partly blocked the synapse loss induced by the LRRTM/NL TKD in NL1 KO neurons, whereas inhibition of both L-type Ca^{2+} channels and NMDA receptors completely abrogated the synapse loss (Figs. 7 [A and B] and S5 C). Next, we treated control and TKD-transfected NL1 KO neurons with the active and inactive enantiomers of a CaM kinase inhibitor (KN-93 and KN-92, respectively, applied for 5 d) and quantified excitatory synapse numbers and sizes (Figs. 7 [C and D] and S5 D). Indeed, chronic blockade of CaM kinase by KN-93 abolished the decrease in excitatory synapse density of LRRTM/NL-deficient neurons, whereas KN-92 had no effect.

The effects of the CaM kinase inhibitor may be a result of a specific inhibition of postsynaptic CaM kinases or of a general impairment of synaptic activity in the cultured neurons. To differentiate between these two possibilities and to test whether a postsynaptic cell-autonomous Ca^{2+}/CaM-dependent signaling pathway mediates synapse loss in LRRTM/NL-deficient neurons, we cotransfected neurons with control plasmid or with TKD and CaM KD plasmids with or without wild-type CaM rescue vectors (see Pang et al., 2010a,b for a detailed description of the CaM KD methodology). Strikingly, KD of CaM abolished the synapse elimination elicited by the TKD of LRRTMs and NLs; this prevention of synapse loss in turn was reversed by expression of wild-type CaM (Figs. 7 [C and D] and S5 D). Because neurons are sparsely infected, CaM acts in a cell-autonomous manner. Thus, synapse elimination induced by loss of LRRTMs and NLs requires a postsynaptic CaM-dependent signaling pathway in the same neurons as those expressing the LRRTM and NL shRNAs.

Discussion

Studies over the last decade established that neurexins, NLs, and LRRTMs function as trans-synaptic cell adhesion molecules and that at least neurexins and NLs are essential for normal brain function (Missler et al., 2003; Chih et al., 2005; Varoqueaux et al., 2006; Linhoff et al., 2009). Moreover, the recent discovery

Downloaded from http://rupress.org/jcb/article-pdf/194/2/323/1894868/jcb_201101072.pdf by guest on 05 December 2025

that both NLs and LRRTMs are postsynaptic ligands for presynaptic neurexins suggested that NLs and LRRTMs act in at least partly overlapping pathways (de Wit et al., 2009; Ko et al., 2009b; Siddiqui et al., 2010). However, two different loss-of-function approaches, mouse KOs versus RNAi-dependent KDs, provided starkly different conclusions about the function of neurexins, NLs, and LRRTMs. Mouse genetics showed that α-neurexins and NLs are essential for survival not because these molecules mediate the establishment of synapses but because they are essential for the functional organization of synapses (Missler et al., 2003; Varoqueaux et al., 2006; Chubykin et al., 2007; Gibson et al., 2009). RNAi experiments, conversely, suggested that neurexins, NLs, and LRRTMs are separately essential for the presence of synapses (Chih et al., 2005; de Wit et al., 2009). Each approach suffers from potential limitations. Whereas noninducible mouse mutants harbor the possibility of developmental compensation, RNAi results are rendered ambiguous by off-target effects and suffer from the difficulty of achieving >80% KD efficiency. In the present study, we have asked whether, under well-controlled conditions in cultured neurons, acute loss of function of multiple LRRTMs and NLs alters the number of synapses and, if so, by which mechanism. In the latter question, we were guided by our earlier observation that NL1 overexpression increases synapse numbers by an activity-dependent pathway (Chubykin et al., 2007), which raised the possibility that NLs and LRRTMs, if they act analogously, may generally regulate synapse maintenance in an activity-dependent manner.

Thus, we asked whether the gain-of-function effects of LRRTMs are also activity dependent and whether loss-of-function effects for NLs and/or LRRTMs are analogously driven by synaptic activity. We made four principal observations: (1) Single KDs of LRRTM1, LRRTM2, and NL3 had no significant effect on synapse numbers in cultured hippocampal neurons; even the combined DKD of LRRTM1 and LRRTM2 or the combined TKD of LRRTM1, LRRTM2, and NL3 did not alter synapse densities. Only the TKD of LRRTM1, LRRTM2, and NL3 applied on the background of the NL1 KO produced a robust decrease in synapse numbers, suggesting that LRRTMs and NLs are functionally redundant, at least as manifested in synapse numbers. (2) Overexpression of either LRRTM2 or NL1 reversed the synapse loss induced by the TKD on the background of the NL1 KO. This reversal was also mediated by LRRTM2 and NL1 mutants that lacked their normal transmembrane regions and cytoplasmic tails, suggesting that the extracellular sequences of these molecules are sufficient for increasing synapse numbers under the TKD/NL1 KO condition. Note that although this experiment looks like a classical rescue experiment, it cannot be interpreted as such because overexpression of these molecules increases synapse numbers in a gain-of-function manner. (3) Strikingly, synapse loss induced by the TKD in NL1 KO neurons was ablated by blocking synaptic activity in cultured neurons. We previously showed that activity blockade prevents the gain-of-function effect of overexpressed NL1 or NL2, but we were surprised that activity blockade also prevents the loss-of-function effects observed here (Chubykin et al., 2007). The fact that activity blockade prevents the synapse loss induced by the NL/LRRTM TKD in NL1 KO neurons indicates that the synapse loss occurs by active synapse elimination and not by lack of synapse formation. Thus, in our arguably most important observation, the loss-of-function decrease in synapse numbers seen here is likely a reflection of a signaling function of LRRTMs and NLs that is required for maintaining normal synapse numbers in active synapses but that is not operational in functionally silent synapses. However, because we globally blocked activity in the cultured neurons, we cannot conclude that under all conditions inactive synapses are protected and never eliminated after NL/LRRTM TKD in NL1 KO neurons. It is conceivable that if only subsets of synapses on a given cell remain active, other rules apply. (4) Finally, in an initial dissection of the signaling pathway involved, we found that inhibition of postsynaptic Ca^{2+} influx, inhibition of CaM kinases, and specific postsynaptic KD of CaM all effectively blocked the synapse elimination induced by the TKD in NL1 KO neurons. The panneuronal inhibition of CaM kinases may have operated by generally dampening synaptic activity, akin to other procedures blocking synaptic activity. However, the effectiveness of the CaM KD is remarkable, given that the KD achieves only a partial suppression of CaM levels (∼70% decrease; Pang et al., 2010a,b) and that the KD was only present in the postsynaptic neurons that were also subject to the TKD. This result implies that Ca^{2+}-dependent postsynaptic activation of CaM is required for synapse elimination induced by the TKD in NL1 KO neurons. Stimulation of specific sets of transcription factors by postsynaptic CaM activation may trigger the TKD phenotype, but the mechanism involved remains to be investigated.

At least three alternative models can be envisioned to account for our results. The first is a synaptic competition model whereby synapses normally compete for each other in an activity-dependent manner in a given neuron, limiting their number. This is the dominant model in current thinking to account for the developmental pruning of synapses and is well supported by extensive studies on neuromuscular and climbing fiber synapses (Rabacchi et al., 1992; Nguyen and Lichtman, 1996; Goda and Davis, 2003; Wyatt and Balice-Gordon, 2003; Cesa and Strata, 2005). However, this model cannot explain our results because a block of synaptic activity itself has no effect on synapse numbers, as our results confirm extensively. Thus, the relative loss of synapses we observe (be it because synapses are eliminated or don't form; see discussion below) is not explained by roles for NLs and LRRTMs in synaptic competition, although this finding does not preclude such a role in more complex in vivo situations.

The second explanation is a synapse capacity model whereby the amount of NLs and LRRTMs determines the number of synapses that are formed and maintained at any given time. The model agrees very well with the overall effects of increased and decreased LRRTM and NL expression on synapse numbers. However, according to this model, the action of LRRTMs and NLs should be activity independent, which is not the case. In particular, the fact that blocking postsynaptic Ca^{2+}/CaM signaling blocks the effect of the LRRTM/NL loss of function on synapse numbers renders this model unlikely.

Downloaded from http://rupress.org/jcb/article-pdf/194/2/323/1894868/jcb_201101072.pdf by guest on 05 December 2025

Third, a synapse elimination model seems most appropriate, whereby synapses are formed independently of synaptic activity. Evidence for this conclusion is also provided by an earlier study showing that synaptic activity is not required for the normal wiring of the brain (Verhage et al., 2000). The synapse elimination model posits that, once formed, synapses are continuously eliminated and reformed in an activity-dependent manner as a "proofreading" mechanism and that the continuous activity-dependent elimination and reformation of synapses require NLs and LRRTMs. This model explains why the absence of NLs and LRRTMs causes activity-dependent synapse elimination, whereas the presence of excess NLs and LRRTMs tips the balance between elimination and reformation to synapse reformation, causing an increased steady-state number of synapses. This model accounts for the puzzling effect that although synapse formation itself is activity independent, refinement of synaptic circuits requires changes in synaptic connectivity that is activity dependent. In this model, NLs and LRRTMs could either be essential for the activity-dependent elimination or reformation of synapses or both, but their absence manifests as an activity-dependent elimination; hence, the title of this paper. To the best of our knowledge, this hypothesis is most consistent with all the available data. It is possible that the function of NLs and LRRTMs in synapse elimination operates normally in developmental synapse pruning or even participates in experience-dependent remodeling of synaptic connectivity, e.g., during learning and memory.

Not surprisingly, our data raise multiple new questions. For example, which proteins direct the initial activity-independent formation of synapses, or how is the number of synapses to be formed determined? How does the Ca^{2+}/CaM-dependent pathway mediate synapse elimination, and why does synaptic activity translate into a loss of synapses instead of a compensatory growth, when NLs and LRRTMs are knocked down? Moreover, it is puzzling that two classes of molecules with no sequence similarity, NLs and LRRTMs, bind to the same presynaptic receptor, neurexins, and are functionally redundant at least in activity-dependent synapse elimination as we describe here. Is this because of their common binding to neurexins and/or a shared postsynaptic signaling pathway? Independent of the answers to these questions, the emerging role for NLs and LRRTMs in the activity-dependent remodeling of synapses promises to provide new avenues for understanding how synapses in the brain are maintained and modified.

Materials and methods

Construction of expression vectors

4 nts (5′-CTACAACTTATAGAGATCCAA-3′ to 5′-CTACCACGTACAGAGACCCAA-3′; the underlined residues were changed) were mutated in pGW1-LRRTM2 mVenus vector to make an shRNA-resistant LRRTM2 expression construct. Residues 38–421 of mouse LRRTM2 (4 nts were mutated) or 46–695 of rat $NL1^{AB}$ were PCR amplified and cloned into pDisplay vector (Invitrogen) by BglII and SalI digestions. pGW1-LRRTM2 mVenus (a mammalian expression vector encoding full-length mouse LRRTM2 fused to mVenus), pCMV5-$NL1^{AB}$ mVenus (a mammalian expression vector encoding full-length rat NL1 splice variant containing inserts in splice sites A and B fused to mVenus), pCMV5-$NL1^{\Delta AB}$ mVenus (a mammalian expression vector encoding full-length rat NL1 splice variant lacking inserts in splice sites A and B fused to mVenus), and pCMV5-NL1-32 mVenus (a mammalian expression vector encoding full-length rat NL1 splice variant lacking inserts in splice sites A and B with five mutated residues critical for neurexin binding fused to mVenus) were previously described (see Fig. 3 A for the structural feature of LRRTM2 or NL1; Boucard et al., 2005; Ko et al., 2009a,b).

Antibodies

The following antibodies were commercially purchased: monoclonal mouse antibody for MAP2 (Sigma-Aldrich), polyclonal guinea pig antibody for vGLUT1 (Millipore), polyclonal rabbit antibody for vesicular γ-aminobutyric acid transporter (VGAT; Millipore), monoclonal antibody for PSD-95 (clone 7E3-1B8; Thermo Fisher Scientific), monoclonal antibody for NMDAR1 (clone M68; Synaptic Systems), polyclonal rabbit antibody for GluR1 (EMD), monoclonal antibody for GluR2 (clone 6C4; Millipore), monoclonal antibody for Rab–GDP dissociation inhibitor (clone 81.2; Synaptic Systems), and polyclonal goat antibody for GFP (Rockland Immunochemicals for Research). Rabbit polyclonal synapsin antibody (E028), polyclonal NL3 antibody (528B), and polyclonal PSD-95 antibody (L667) were previously described (Irie et al., 1997; Chubykin et al., 2005; Tabuchi et al., 2007).

Generation of lentiviral shRNA plasmids

To construct the shRNA lentivirus expression vectors, the oligonucleotides targeting mouse LRRTMs (LRRTM1 and LRRTM2) or mouse NL3 were annealed, phosphorylated, and subcloned into XhoI and XbaI sites of a single KD vector (see Fig. 1 A for the schematic diagram of vectors) immediately downstream of the human H1 promoter. For an LRRTM DKD, the oligonucleotides containing LRRTM1 (J14) and LRRTM2 (J17 and J18; for DKD vector) were subcloned into the XhoI–XbaI (J14), AscI–RsrII (J17), and BstEII–BsiWI (J18) sites. For a TKD vector, the oligonucleotides containing J14, J17, J18, and NL3 (J50) sequences were subcloned into the XhoI–XbaI (J14), AscI–RsrII (J17), BstEII–BsiWI (J18), and SbfI–BstBI (J50) sites of a TKD vector that contains two human H1 promoters and two human U6 promoters. Note that the sequence in LRRTM2 (J33) was reported to be potent in knocking down LRRTM2 proteins (de Wit et al., 2009) and used in parallel with the other LRRTM shRNA vectors in this study (Fig. 1 B). The nucleotide target sequences are as follows (the linker sequences were omitted here; sequences that did not work are not included): LRRTM1 (J14), 5′-CAGCCTCAAGTTTCTCGACAT-3′; LRRTM2 (J17), 5′-GCTACAACTTATAGAGATCCA-3′; LRRTM2 (J18), 5′-CCAGTATAAGAAGTAGACTTA-3′; LRRTM2 (J33), 5′-TGCTATTCTACTGCGACTCTC-3′; and NL3 (J50), 5′-GCAGTGTTCTTGCAAGTTA-3′.

Production and characterization of recombinant lentiviruses

Recombinant lentiviruses were produced by transfection of human embryonic kidney 293T cells with four plasmids, single KD or LRRTM DKD or TKD vectors pRRE, pVSVg, and pREV, using FuGENE-6 reagent (Roche) as previously described (Maximov et al., 2009). pRRE, pVSVg, and pREV encode the elements essential for packaging viral particles. Viruses were harvested 48 h after transfection by collecting the media from transfected HEK293T cells, and brief centrifugation at 1,000 *g* was performed to remove cellular debris. Cultured mouse cortical neurons were infected with 350 µl of conditioned cell medium for each 24-well tissue culture dish of high-density neurons at DIV4 or 5 and harvested at DIV12 or 13 for quantitative RT-PCR analyses using the TaqMan assay kit (Applied Biosystems). The following probes for quantitative RT-PCR analyses were purchased from Applied Biosystems: LRRTM1 (Mm00551337_g1), LRRTM2 (Mm00997210_g1), LRRTM3 (Mm00618457_m1), LRRTM4 (Mm01185896_m1), NL3 (Mm01225951_m1), and glyceraldehyde 3-phosphate dehydrogenase (for normalization).

Primary neuronal culture, transfections, immunocytochemistry, image acquisition, and analyses

At postnatal day 0 (P_0), mouse pups were used to prepare cortical or hippocampal cultures as previously described (Ko et al., 2009a). In brief, primary tissues from either the cortex or hippocampus from P_0 pups were dissociated by papain digestion for 20 min at 37°C and plated on poly-D-lysine–coated glass coverslips. NL1 KO was previously described (Varoqueaux et al., 2006). For RNAi experiments, cultured mouse hippocampal neurons (derived from either wild-type or NL1 KO) were transfected by the calcium phosphate method with lentiviral shRNA vectors at DIV3 or 9 and immunostained at DIV14 by the antibodies as indicated in the figure legends. For infection experiments (Fig. S2, A and B), the hippocampal cultured neurons were infected at DIV3 with the indicated lentiviruses and immunostained at DIV14. Mouse hippocampal neurons at DIV9 or 10 were treated with single or multiple receptor antagonists or a channel blocker (L-type calcium channel blocker = 10 µM nifedipine; NMDA receptor antagonist = 50 µM APV; non-NMDA receptor antagonist = 20 µM NBQX; type II metabotropic glutamate receptor antagonist = 10 µM LY341495; γ-aminobutyric acid receptor antagonist = 50 µM picrotoxin; sodium channel blocker = 2 µM TTX; CaM kinase inhibitor and its inactive analogue = 5 µM KN-93 and KN-92; and DMSO [negative control]).

Downloaded from http://rupress.org/jcb/article-pdf/194/2/323/1894868/jcb_201101072.pdf by guest on 05 December 2025

The transfected or infected neurons were fixed with 4% PFA/4% sucrose for 10 min at room temperature, permeabilized with 0.2% Triton X-100 in PBS for 5 min at 4°C, blocked with 3% horse serum/0.1% crystalline-grade BSA in PBS for 30 min at room temperature, and incubated with the indicated primary and secondary antibodies in blocking solution for 1 h at room temperature, respectively. Surface AMPA receptors were labeled in live neurons by a 15-min incubation at 37°C with polyclonal GluR1 antibody (1:20 in conditioned media, i.e., MEM + 0.5 mM glutamax I; EMD) directed against the N terminus of the GluR1 receptor subunit as previously described (Beattie et al., 2000), followed by fixation and incubation with donkey anti–rabbit Cy3-conjugated secondary antibodies. The following antibodies were used in conventional immunocytochemistry experiments: GFP (1:500), MAP2 (1:2,000), synapsin (1:1,000), vGLUT1 (1:1,000), VGAT (1:500), NMDAR1 (1:100), GluR2 (1:150), and PSD-95 (1:500). The transfected or infected neurons were randomly chosen and acquired using a confocal microscope (LSM510; Carl Zeiss) with 10 or 63× objective lenses (0.3 and 1.4 NAs, respectively), and all of the image settings were kept constant. Z-stacked images obtained from confocal microscopy were converted to maximal projection and analyzed using MetaMorph software (Molecular Devices) with size and density of spines and presynaptic terminals. All of the images were separated with different color channels (red and green), and red-colored images were transformed into an image by grayscale mode in Photoshop (Adobe). After selecting one or two primary dendrites from neurons in a single image frame, the dendrite lengths were recorded, and dendritic regions of interest were manually traced in MetaMorph software and saved for puncta measurements (in a format of rgn files). The constant intensity threshold such that diffuse nonsynaptic signals are excluded but synaptic signals are included (threshold set level = 90 in the range of 0–255) was applied to all gray images. The saved dendritic regions were loaded, calibrated, and measured by the integrated morphometry analysis menu. For linear density of synapses, the total puncta numbers calculated were normalized to 1/50 µm dendrite. For spine number measurements, total dendritic protrusions (~0.5–3.0-µm length) were manually counted in selected dendrites identified by filling GFP signal and normalized. For synapse size measurement, the normalized puncta areas were calculated and exported automatically to Excel (Microsoft).

Electrophysiology

Coverslips were transferred to a submerged recording chamber perfused with artificial cerebrospinal fluid at room temperature (22–25°C) consisting of 122 mM NaCl, 26 mM $NaHCO_3$, 11 mM glucose, 2.5 mM KCl, 2 mM $CaCl_2$, 2 mM $MgSO_4$, and 1 mM NaH_2PO_4. Evoked EPSCs (AMPA or NMDA receptor mediated) and IPSCs were recorded from voltage-clamped neurons using one of two internal solutions. For EPSC experiments, the patch pipette contained 117.5 mM Cs-methanesulfonate, 15.5 mM CsCl, 10 mM tetraethyl ammonium–Cl, 8 mM NaCl, 10 mM Hepes, 10 mM Na-phosphocreatine, 1 mM $MgCl_2$, 4 mM ATP-Mg, 0.3 mM GTP-Na, 5 mM EGTA, and 1 mM QX-314. For IPSC recordings, the internal solution was identical to the one used for EPSCs except that Cs-methanesulfonate and CsCl were 95 mM and 55 mM, respectively. Holding potentials were as follows: AMPA-EPSC and IPSCs at –70 mV and NMDA-EPSCs at 40 mV. Electrode resistances ranged from 2 to 4 MΩ, and series resistances were 6–12 MΩ after obtaining whole-cell configuration. Synaptic responses were elicited by single 90-µA/100-µs current injections (0.1 Hz) via a concentric bipolar electrode placed ~150 µm away from the soma using a stimulus isolation unit (ISO-Flex; A.M.P.I.). Care was taken to avoid placing the electrode over the dendritic field of the recorded neurons. EPSCs were pharmacologically isolated by adding 50 µM picrotoxin and either 50 µM APV (NMDA receptor antagonist) or 10 µM NBQX (non-NMDA receptor antagonist) to the external solution. IPSCs were isolated by blocking excitation with both APV and NBQX. Recordings were performed using an amplifier (Multiclamp 700B; Molecular Devices) and custom software written in IGOR Pro (Wavemetrics), digitized at 10 KHz, filtered at 5 KHz, and analyzed in IGOR Pro.

Statistics

Statistical significance was determined by a Student's *t* test only when two values were compared. Otherwise, an analysis of variance (ANOVA) Tukey's test was used for statistics. For electrophysiology data, unpaired and two-tailed Student's *t* tests were used. All data shown are means ± SEMs, and numerical values for morphometric results are listed in Table S1.

Online supplemental material

Fig. S1 shows an example of raw quantitative RT-PCR curves to demonstrate NL3 KD efficiency and immunoblots to document NL3 protein reductions. Fig. S2 shows a comparative analysis of synapse numbers in wild-type mouse hippocampal neurons that are either transfected with control or LRRTM2 DKD vectors or that are infected with control or LRRTM DKD lentiviruses. In addition, Fig. S2 displays additional analyses of the TKD effects in cultured NL1 KO hippocampal neurons with various pre- and postsynaptic markers (in particular, analyses of synapse sizes). Fig. S3 describes the quantitative analysis of neuronal size and dendritic arborization in control NL1 KO and TKD-treated NL1 KO neurons that were stained for a somatodendritic marker (MAP2). This figure also shows representative images and synapse size analyses of NL1 KO neurons that were transfected with control and TKD plasmids and analyzed for extended time periods (DIV14, DIV17, and DIV20). Fig. S4 depicts representative images of the effects of activity blockers on synapse numbers and an analysis of chronic stimulation of neurons with 15 mM KCl on synapse numbers and sizes (all in control and TKD NL1 KO neurons). Fig. S5 shows nonmerged images corresponding to the merged images of Fig. 6 and displays analyses of synapses sizes complementing the analyses of synapse densities shown in Figs. 6 and 7. Table S1 summarizes the numerical values obtained from the morphology experiments in this paper, as depicted in the main and supplemental figures, to allow independent assessment of raw data. Online supplemental material is available at http://www.jcb.org/cgi/content/full/jcb.201101072/DC1.

We thank Dr. Zhiping P. Pang for initial development of multiple shRNA vectors.

Our work was supported by grants from the National Institute of Mental Health (to T.C. Südhof and R.C. Malenka) and the Simons Foundation (to T.C. Südhof) and by a fellowship from the International Human Frontier Science Program Organization (to J. Ko; LT00021/2008-L) and a National Research Service Award from the National Institute of Mental Health (to M.V. Fuccillo; MH086176-02).

Submitted: 14 January 2011
Accepted: 22 June 2011

References

Alvarez, V.A., D.A. Ridenour, and B.L. Sabatini. 2006. Retraction of synapses and dendritic spines induced by off-target effects of RNA interference. *J. Neurosci.* 26:7820–7825. doi:10.1523/JNEUROSCI.1957-06.2006

Beattie, E.C., R.C. Carroll, X. Yu, W. Morishita, H. Yasuda, M. von Zastrow, and R.C. Malenka. 2000. Regulation of AMPA receptor endocytosis by a signaling mechanism shared with LTD. *Nat. Neurosci.* 3:1291–1300. doi:10.1038/81823

Boucard, A.A., A.A. Chubykin, D. Comoletti, P. Taylor, and T.C. Südhof. 2005. A splice code for *trans*-synaptic cell adhesion mediated by binding of neuroligin 1 to α- and β-neurexins. *Neuron*. 48:229–236. doi:10.1016/j.neuron.2005.08.026

Budreck, E.C., and P. Scheiffele. 2007. Neuroligin-3 is a neuronal adhesion protein at GABAergic and glutamatergic synapses. *Eur. J. Neurosci.* 26:1738–1748. doi:10.1111/j.1460-9568.2007.05842.x

Cesa, R., and P. Strata. 2005. Axonal and synaptic remodeling in the mature cerebellar cortex. *Prog. Brain Res.* 148:45–56. doi:10.1016/S0079-6123(04)48005-4

Chih, B., H. Engelman, and P. Scheiffele. 2005. Control of excitatory and inhibitory synapse formation by neuroligins. *Science*. 307:1324–1328. doi:10.1126/science.1107470

Chubykin, A.A., X. Liu, D. Comoletti, I. Tsigelny, P. Taylor, and T.C. Südhof. 2005. Dissection of synapse induction by neuroligins: effect of a neuroligin mutation associated with autism. *J. Biol. Chem.* 280:22365–22374. doi:10.1074/jbc.M410723200

Chubykin, A.A., D. Atasoy, M.R. Etherton, N. Brose, E.T. Kavalali, J.R. Gibson, and T.C. Südhof. 2007. Activity-dependent validation of excitatory versus inhibitory synapses by neuroligin-1 versus neuroligin-2. *Neuron*. 54:919–931. doi:10.1016/j.neuron.2007.05.029

de Wit, J., E. Sylwestrak, M.L. O'Sullivan, S. Otto, K. Tiglio, J.N. Savas, J.R. Yates III, D. Comoletti, P. Taylor, and A. Ghosh. 2009. LRRTM2 interacts with Neurexin1 and regulates excitatory synapse formation. *Neuron*. 64:799–806. doi:10.1016/j.neuron.2009.12.019

Francks, C., S. Maegawa, J. Laurén, B.S. Abrahams, A. Velayos-Baeza, S.E. Medland, S. Colella, M. Groszer, E.Z. McAuley, T.M. Caffrey, et al. 2007. LRRTM1 on chromosome 2p12 is a maternally suppressed gene that is associated paternally with handedness and schizophrenia. *Mol. Psychiatry*. 12:1129–1139: 1057. doi:10.1038/sj.mp.4002053

Gibson, J.R., K.M. Huber, and T.C. Südhof. 2009. Neuroligin-2 deletion selectively decreases inhibitory synaptic transmission originating from fast-spiking but not from somatostatin-positive interneurons. *J. Neurosci.* 29:13883–13897. doi:10.1523/JNEUROSCI.2457-09.2009

Downloaded from http://rupress.org/jcb/article-pdf/194/2/323/1894868/jcb_201101072.pdf by guest on 05 December 2025

Goda, Y., and G.W. Davis. 2003. Mechanisms of synapse assembly and disassembly. *Neuron*. 40:243–264. doi:10.1016/S0896-6273(03)00608-1

Graf, E.R., X. Zhang, S.X. Jin, M.W. Linhoff, and A.M. Craig. 2004. Neurexins induce differentiation of GABA and glutamate postsynaptic specializations via neuroligins. *Cell*. 119:1013–1026. doi:10.1016/j.cell.2004.11.035

Ichtchenko, K., Y. Hata, T. Nguyen, B. Ullrich, M. Missler, C. Moomaw, and T.C. Südhof. 1995. Neuroligin 1: a splice site-specific ligand for β-neurexins. *Cell*. 81:435–443. doi:10.1016/0092-8674(95)90396-8

Irie, M., Y. Hata, M. Takeuchi, K. Ichtchenko, A. Toyoda, K. Hirao, Y. Takai, T.W. Rosahl, and T.C. Südhof. 1997. Binding of neuroligins to PSD-95. *Science*. 277:1511–1515. doi:10.1126/science.277.5331.1511

Ko, J., C. Zhang, D. Arac, A.A. Boucard, A.T. Brunger, and T.C. Südhof. 2009a. Neuroligin-1 performs neurexin-dependent and neurexin-independent functions in synapse validation. *EMBO J.* 28:3244–3255. doi:10.1038/emboj.2009.249

Ko, J., M.V. Fuccillo, R.C. Malenka, and T.C. Südhof. 2009b. LRRTM2 functions as a neurexin ligand in promoting excitatory synapse formation. *Neuron*. 64:791–798. doi:10.1016/j.neuron.2009.12.012

Laurén, J., M.S. Airaksinen, M. Saarma, and T. Timmusk. 2003. A novel gene family encoding leucine-rich repeat transmembrane proteins differentially expressed in the nervous system. *Genomics*. 81:411–421. doi:10.1016/S0888-7543(03)00030-2

Linhoff, M.W., J. Laurén, R.M. Cassidy, F.A. Dobie, H. Takahashi, H.B. Nygaard, M.S. Airaksinen, S.M. Strittmatter, and A.M. Craig. 2009. An unbiased expression screen for synaptogenic proteins identifies the LRRTM protein family as synaptic organizers. *Neuron*. 61:734–749. doi:10.1016/j.neuron.2009.01.017

Maximov, A., Z.P. Pang, D.G. Tervo, and T.C. Südhof. 2007. Monitoring synaptic transmission in primary neuronal cultures using local extracellular stimulation. *J. Neurosci. Methods*. 161:75–87. doi:10.1016/j.jneumeth.2006.10.009

Maximov, A., J. Tang, X. Yang, Z.P. Pang, and T.C. Südhof. 2009. Complexin controls the force transfer from SNARE complexes to membranes in fusion. *Science*. 323:516–521. doi:10.1126/science.1166505

Missler, M., W. Zhang, A. Rohlmann, G. Kattenstroth, R.E. Hammer, K. Gottmann, and T.C. Südhof. 2003. Alpha-neurexins couple Ca^{2+} channels to synaptic vesicle exocytosis. *Nature*. 423:939–948. doi:10.1038/nature01755

Nguyen, Q.T., and J.W. Lichtman. 1996. Mechanism of synapse disassembly at the developing neuromuscular junction. *Curr. Opin. Neurobiol.* 6:104–112. doi:10.1016/S0959-4388(96)80015-8

Pang, Z.P., P. Cao, W. Xu, and T.C. Südhof. 2010a. Calmodulin controls synaptic strength via presynaptic activation of calmodulin kinase II. *J. Neurosci.* 30:4132–4142. doi:10.1523/JNEUROSCI.3129-09.2010

Pang, Z.P., W. Xu, P. Cao, and T.C. Südhof. 2010b. Calmodulin suppresses synaptotagmin-2 transcription in cortical neurons. *J. Biol. Chem.* 285:33930–33939. doi:10.1074/jbc.M110.150151

Poulopoulos, A., G. Aramuni, G. Meyer, T. Soykan, M. Hoon, T. Papadopoulos, M. Zhang, I. Paarmann, C. Fuchs, K. Harvey, et al. 2009. Neuroligin 2 drives postsynaptic assembly at perisomatic inhibitory synapses through gephyrin and collybistin. *Neuron*. 63:628–642. doi:10.1016/j.neuron.2009.08.023

Rabacchi, S., Y. Bailly, N. Delhaye-Bouchaud, and J. Mariani. 1992. Involvement of the N-methyl D-aspartate (NMDA) receptor in synapse elimination during cerebellar development. *Science*. 256:1823–1825. doi:10.1126/science.1352066

Siddiqui, T.J., R. Pancaroglu, Y. Kang, A. Rooyakkers, and A.M. Craig. 2010. LRRTMs and neuroligins bind neurexins with a differential code to cooperate in glutamate synapse development. *J. Neurosci.* 30:7495–7506. doi:10.1523/JNEUROSCI.0470-10.2010

Song, J.Y., K. Ichtchenko, T.C. Südhof, and N. Brose. 1999. Neuroligin 1 is a postsynaptic cell-adhesion molecule of excitatory synapses. *Proc. Natl. Acad. Sci. USA*. 96:1100–1105. doi:10.1073/pnas.96.3.1100

Sousa, I., T.G. Clark, R. Holt, A.T. Pagnamenta, E.J. Mulder, R.B. Minderaa, A.J. Bailey, A. Battaglia, S.M. Klauck, F. Poustka, and A.P. Monaco. 2010. Polymorphisms in leucine-rich repeat genes are associated with autism spectrum disorder susceptibility in populations of European ancestry. *Mol. Autism*. 1:7.

Südhof, T.C. 2008. Neuroligins and neurexins link synaptic function to cognitive disease. *Nature*. 455:903–911. doi:10.1038/nature07456

Tabuchi, K., J. Blundell, M.R. Etherton, R.E. Hammer, X. Liu, C.M. Powell, and T.C. Südhof. 2007. A neuroligin-3 mutation implicated in autism increases inhibitory synaptic transmission in mice. *Science*. 318:71–76. doi:10.1126/science.1146221

Ushkaryov, Y.A., A.G. Petrenko, M. Geppert, and T.C. Südhof. 1992. Neurexins: synaptic cell surface proteins related to the alpha-latrotoxin receptor and laminin. *Science*. 257:50–56. doi:10.1126/science.1621094

Varoqueaux, F., S. Jamain, and N. Brose. 2004. Neuroligin 2 is exclusively localized to inhibitory synapses. *Eur. J. Cell Biol.* 83:449–456. doi:10.1078/0171-9335-00410

Varoqueaux, F., G. Aramuni, R.L. Rawson, R. Mohrmann, M. Missler, K. Gottmann, W. Zhang, T.C. Südhof, and N. Brose. 2006. Neuroligins determine synapse maturation and function. *Neuron*. 51:741–754. doi:10.1016/j.neuron.2006.09.003

Verhage, M., A.S. Maia, J.J. Plomp, A.B. Brussaard, J.H. Heeroma, H. Vermeer, R.F. Toonen, R.E. Hammer, T.K. van den Berg, M. Missler, et al. 2000. Synaptic assembly of the brain in the absence of neurotransmitter secretion. *Science*. 287:864–869. doi:10.1126/science.287.5454.864

Wayman, G.A., Y.S. Lee, H. Tokumitsu, A.J. Silva, and T.R. Soderling. 2008. Calmodulin-kinases: modulators of neuronal development and plasticity. *Neuron*. 59:914–931. (published erratum appears in *Neuron*. 2009. 64:590) doi:10.1016/j.neuron.2008.08.021

Wyatt, R.M., and R.J. Balice-Gordon. 2003. Activity-dependent elimination of neuromuscular synapses. *J. Neurocytol.* 32:777–794. doi:10.1023/B:NEUR.0000020623.62043.33

Downloaded from http://rupress.org/jcb/article-pdf/194/2/323/1894868/jcb_201101072.pdf by guest on 05 December 2025